

The impact of the SKA on Galactic Radioastronomy: continuum observations

Grazia Umama^{*1}, Corrado Trigilio¹, Luciano Cerrigone², Riccardo Cesaroni³, Albert A. Zijlstra⁴, Melvin Hoare⁵, Kerstin Weis⁶, Anthony J. Beasley⁷, Dominik Bomans⁶, Greg Hallinan⁸, Sergio Molinari⁹, Russ Taylor¹⁰, Leonardo Testi¹¹, Mark Thompson¹²,

¹INAF OACT, Catania, Italy; ²JCentro de Astrobiologia (INTA-CSIC), Madrid, Spain; ³INAF Osservatorio Astrofisico di Arcetri, Firenze Italy; ⁴Jodrell Bank Centre for Astrophysics, Manchester M13 9PL, UK; ⁵University of Leeds, Leeds, UK; ⁶Astronomisches Institut, Ruhr-Universitaet, Bochum, Germany; ⁷National Radio Astronomy Observatory, Charlottesville, USA; ⁸Department of Astronomy, California Institute of Technology, Pasadena, CA 91125, USA; ⁹INAF IAPS, Roma, Italy; ¹⁰ University of Cape Town and The University of the Western Cape, SA; ¹¹ ESO, Karl Schwarzschild str. 2, D-85748 Garching, Germany; ¹²University of Hertfordshire, UK

E-mail: Grazia.Umana@oact.inaf.it

The SKA will be a state of the art radiotelescope optimized for both large area surveys as well as for deep pointed observations. In this paper we analyze the impact that the SKA will have on Galactic studies, starting from the immense legacy value of the all-sky survey proposed by the continuum SWG but also presenting some areas of Galactic Science that particularly benefit from SKA observations both surveys and pointed.

The planned all-sky survey will be characterized by unique spatial resolution, sensitivity and survey speed, providing us with a wide-field atlas of the Galactic continuum emission. Synergies with existing, current and planned radio Galactic Plane surveys will be discussed. SKA will give the opportunity to create a sensitive catalog of discrete Galactic radio sources, most of them representing the interaction of stars at various stages of their evolution with the environment: complete census of all stage of HII regions evolution; complete census of late stages of stellar evolution such as PNe and SNRs; detection of stellar winds, thermal jets, Symbiotic systems, Chemically Peculiar and dMe stars, active binary systems in both flaring and quiescent states. Coherent emission events like Cyclotron Maser in the magnetospheres of different classes of stars can be detected. Pointed, deep observations will allow new insights into the physics of the coronae and plasma processes in active stellar systems and single stars, enabling the detection of flaring activity in larger stellar population for a better comprehension of the mechanism of energy release in the atmospheres of stars with different masses and age.

Advancing Astrophysics with the Square Kilometre Array
June 8-13, 2014
Giardini Naxos, Italy

*Speaker.

1. The all-sky SKA1 survey

The proposed SKA1 all sky continuum survey (SASS1: Norris et al. 2015), covering most ($\sim 70\%$) of the Galactic Plane with unprecedented spatial resolution, sensitivity and survey speed at band 2 (650-1670 MHz), will provide us with a sensitive wide-field atlas of Galactic continuum emission. Up to now, existing interferometric radio continuum surveys of the Galactic Plane have been carried out either at high angular resolution, but over a limited survey area, or over wider areas but at low angular resolution. This is the case of MAGPIS (Helfand et al., 2006) and CORNISH surveys (Hoare et al., 2012), covering an area of \sim square degrees at an angular resolution of 1-6". On the other side, the International Galactic Plane Survey (McClure-Griffiths et al., 2005; Taylor et al., 2003) and the 2nd Epoch Molonglo Galactic Plane Surveys (MGPS-2: Murphy et al., 2007) cover several hundred square degrees at a typical resolution of ~ 1 arcmin.

In the meantime, two major surveys including or aimed at mapping the Galactic Plane will be carried out by the two SKA precursors, namely: the Evolutionary Map of the Universe (EMU, Norris et al., 2011) a deep ($\sim 10\mu\text{Jy}/\text{beam}$), almost full sky (75%), $\sim 10''$ angular resolution survey to be carried out at 1.4 GHz with the Australian SKA Pathfinder (ASKAP); and MeerGal (PIs M. Thompson and S. Goedhart) a deep ($\sim 30\mu\text{Jy}/\text{beam}$) survey of the Milky Way Galaxy (140 square degrees) to be carried out at 14 GHz with MeerKAT at a sub-arcsec ($\sim 0.8''$) angular resolution.

We can anticipate that both surveys will provide us with a new view of the radio Galactic Plane. However, SASS1, due to the increase in sensitivity, angular resolution and survey speed, will bridge the gap between the two types of existing radio surveys of the Galactic Plane and will improve the results from EMU and MeerGAL, detecting and cataloguing objects such as HII regions, supernova remnants (SNRs), planetary nebulae (PNe) and radio stars, down to the μJy level. Most of these sources represent the interaction of stars at various stages of evolution with their environment. The known radio populations of each of these types of objects are limited by a combination of issues including the limited area covered by existing surveys, sensitivity, angular resolution or biases against large scale structures introduced by limited uv coverage snapshot surveys. Moreover, the lessons learnt from EMU will guide the SASS1 design in identifying issues arising from the complex continuum structure associated with the Galactic Plane and from the variable sources in the Galactic Plane.

However, besides the legacy value of SASS1, some areas of Galactic Science will particularly benefit from SKA observations, in particular from those conducted at higher frequencies (band 4 and/or 5) and at higher resolution (sub-arcsec). We will present some among the possible Galactic science goals that can be addressed with the SKA1 and the full SKA. In the following, we assume the SKA1 and SKA performances as reported in the SKA1 Baseline Design (Dewdney et al., 2013) and in the Performance Memo (Braun, 2014).

2. Massive star formation

A straightforward application of SKA will be the study of ionized regions around massive, early-type stars. Thanks to its overwhelming sensitivity and dynamic range SKA will be the ideal instrument to detect and resolve these objects, whose size may vary from 10^3 au, for hypercompact

(HC) HII regions, to 100 pc, for giant HII regions. This is equivalent to span a broad range of ages, as HII regions are known to expand with time, which makes SKA an excellent tool to investigate the evolution of these intriguing objects.

While the most extended (and hence old) stages can be (and have effectively been) studied with the Very Large Array, the youngest sources have been so far quite elusive. The HC HII regions may be as small as <0.03 pc, which turns into an angular size $< 1''$ at the typical distances of OB-type stars (>1 kpc). Such a small size, combined with the large opacity of the free-free emission in the radio regime, makes it challenging to detect this type of objects and even more to resolve them. The limited information available on the earliest evolution of HII regions is frustrating, as this is considered a crucial step in the formation of a high-mass star (Keto, 2003). The youngest, densest HII regions arise as the star contracts towards its main sequence configuration. As long as accretion at high rates goes on, the protostar may swell up (Hosokawa et al., 2010) and cool down, thus dramatically reducing the ionizing photon output. This implies that the appearance of an HC HII region must correspond to the termination of the main accretion phase. In this context, the morphology of the youngest HIIs tells us also about the distribution of material immediately surrounding the forming massive star in terms of the interaction between infall and outflow.

As a matter of fact, HII regions appear to remain in the most compact phases of their evolution longer than expected on the basis of a simple expansion model, as witnessed by the number of ultracompact HII regions in the Galaxy (Wood & Churchwell, 1989; Mottram et al., 2011). This result implies the existence of some confinement, which could be tightly related to the accretion mechanism itself, as shown by Keto (2002). Alternatively, effects of density gradients and stellar winds may play a role (Arthur & Hoare, 2006) or intrinsic variability driven by changes in the accretion rate (De Pree et al., 2014). Therefore, shedding light on the earliest phases of HII regions might be equivalent to unveiling the process of high-mass star formation.

What is needed to boost our knowledge of (hypercompact) HII regions is both a statistically complete sample and a detailed analysis of selected candidates. Note also that radio observations should be better performed at higher frequencies, as this regime is well suited to actually determine the morphology of the youngest, most compact HII regions. SKA can fulfil all of these requirements, thanks to its superior sensitivity, angular resolution, and frequency coverage. The sensitivity issue is illustrated in Fig. 1, where we show the detection limits of SKA1 and SKA. In our estimate we have assumed a classical (Strömgren) HII region ionized by a zero-age main-sequence star. The figures plot the intensity of an HII region as a function of the Strömgren radius and Lyman continuum of the ionizing star. The curves correspond to the 3σ level attainable with 10 min integration on-source at 9 GHz with $1''$ resolution, for a source distance of 1 kpc (solid line) and 20 kpc (dashed). The HII regions falling above the curve are detectable. One sees that even SKA1 will be sensitive enough to detect HII regions as small as a few 10 au (the size of our Solar system!) around a B2 star or earlier, across the whole Galaxy. The great potential of SKA will permit to perform unbiased surveys of the Galactic plane in a limited amount of time and with great sensitivity, and thus allow a complete census of Galactic hypercompact (besides more extended) HII regions.

Resolving a HC HII region is more challenging. The maximum diameter is ~ 0.03 pc (Kurtz, 2005) (i.e. $0.6''$ at a distance of, e.g., 10 kpc) and requires a synthesized beam at least ~ 10 times smaller (i.e. $<0.06''$) to be properly imaged. In Fig. 2 we show a plot analogous to those in Fig. 1, but this time we fix the ratio between the synthesized beam and the source angular diameter to

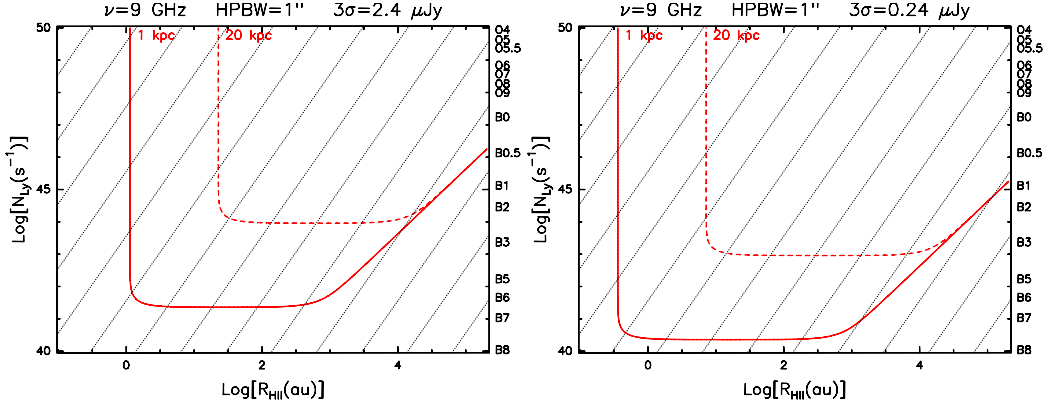


Figure 1: Left: Plot of the peak free-free continuum flux density of an homogenous, isothermal (Strömgen) HII region as a function of the HII region radius and Lyman continuum photon rate of the ionizing star. The calculation has been performed assuming an observing frequency of 9 GHz and an angular resolution of $1''$. The two curves correspond to a 3σ detection level of $2.4 \mu\text{Jy}$ (obtainable in 10 min on-source with SKA1) at a distance of 1 kpc (solid curve) and 20 kpc (dashed). The dotted lines correspond to fixed values of the HII region densities, ranging from 10^{-1} cm^{-3} in the bottom right to 10^{12} cm^{-3} in the top right, in steps of a factor 10. **Right:** Same as left panel, for a detection threshold of $0.24 \mu\text{Jy}$, attainable with SKA in 10 minute integration on-source.

10. The curves correspond to $S/N=10$ for 10 min integration on-source, assuming a 1σ RMS of $0.08 \mu\text{Jy}$ for SKA at 9 GHz. Points above the solid blue line have electron densities in excess of 10^6 cm^{-3} , the minimum value for a HC HII region (see Kurtz 2005). We conclude that the SKA will resolve HC HII regions around B1 stars or earlier, all over the Galaxy.

In addition to the sensitivity and angular resolution, SKA will provide us also with a broad instantaneous frequency coverage, thus allowing us to measure the spectral index of the radio emission. Although not sufficient by itself, knowledge of the spectral slope is a crucial piece of information to discriminate between HII regions and thermal jets, and determine the optical depth of the emission. Indeed, radio jets might be confused with faint HII regions and are detectable even at large distances (see Anglada et al. 2015).

3. Late stages of stellar evolution

SKA will also contribute to unveil the so-far missed populations of Planetary Nebulae (PNe) and Supernova remnants (SNRs). Those objects represent the late stages of stellar evolution of low and intermediate mass stars and massive stars, respectively. Details on the potential of SKA on SNRs science can be found in Wang et al. (2015). Low and intermediate mass stars (LIMS: $0.8\text{--}8 M_{\odot}$) constitute 90% of all stars which have died in the Universe. During their final evolution, these stars eject between 40% and 80% of their total mass, enriched by the products of nucleosynthesis. The ejecta are the source of half the recycled gas in the Galaxy and are major contributors to chemical evolution of the Galaxy. The mass loss also determines the final mass of stellar remnants. The mass-loss process is one the main open problems in stellar astrophysics. Current areas

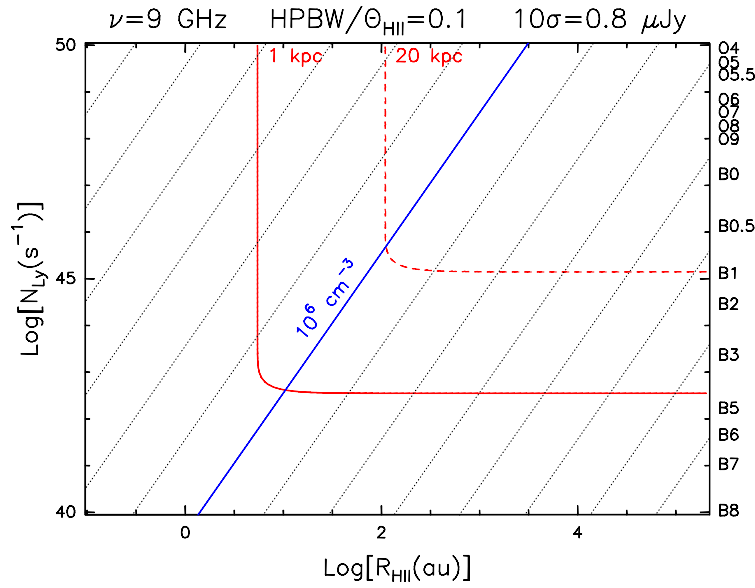


Figure 2: Same as previous figure. The difference is that here we fix the ratio between synthesized beam and source angular diameter diameter to 0.1 and allow for a $S/N=10$ for an integration of 10 min on-source with SKA (resulting in $1\sigma \simeq 0.08 \mu\text{Jy}$). The blue line corresponds to an HII region density of 10^6 cm^{-3} .

of research are: what drives the mass loss, how is it affected by binary interactions and magnetic fields, and whether there is a unique initial-final mass relation.

Planetary nebulae (PNe) are formed when the ejecta are briefly ionized by the stellar remnant; they are known for their often beautiful morphologies. Since they have a rich emission-line spectrum, they can also be used to trace the kinematics of their host galaxies as well as serve as standard candles (e.g. Ciardullo, 2010). Although they trace 90% of all stars, they are short-lived (a few 10^4 yr), hence relatively rare, with a population density $\sim 10^{-6}$ of that of the total stellar population. This is compensated by their high luminosity ($\sim 10^4 L_{\odot}$).

PNe are among the most numerous Galactic radio sources detected so far in radio surveys (about 700 in the NVSS). However, our census of this type of stars is far below the number expected from theoretical counts, which, on the other hand, heavily depend on the assumptions on the previous evolution of the stars. If, for example, only binary interaction is required to form a PN, we can expect to observe ~ 6600 PNe in our Galaxy, but this number can go up to ~ 46000 , if binaries are not strictly necessary (Jacoby et al., 2010). The number of detected Galactic PNe is only ~ 3000 (Parker et al., 2006).

It is therefore possible that there is a missing population of PNe. The main reason for such a large mismatch between the expected and the observed number of sources is that most PNe are hidden by dust absorption. Among other factors that can hamper PN detections, there are the intrinsic low brightness of the more evolved sources, which numerically dominate the PN luminosity function and are then expected to constitute the main component of volume-limited samples (Parker et al., 2006), the interaction with the ISM, which can disrupt the nebulae and shorten their lives, and the fact that Galactic latitudes beyond ± 10 deg have not been adequately surveyed (Jacoby et al., 2010).

The sensitivity of the SKA and its ability to map large areas of the sky quickly will allow us to detect every PN in the Milky Way. If we consider a typical expansion velocity of 10 km s^{-1} , the shell expands in $2 \times 10^4 \text{ yr}$ to a distance of about 0.2 pc from the central star. Assuming optically thin emission from an ionised mass of $0.1 M_{\odot}$ ($n_e \sim 140 \text{ cm}^{-3}$) filling 2/3 of the shell, we expect a flux density of about $4 \mu\text{Jy}/\text{beam}$ at a distance of 61 kpc, over a beam of $0.8''$. This means that SKA1 will be able to detect and map evolved PNe not only in the whole Galaxy, but also in the Magellanic Clouds. The number counts, distribution and brightness temperature will test the mass-loss models of LIMS. This survey can be done at frequencies between 1 and 5 GHz, with lower confusion and less effect from optical depth (for the younger nebulae) at the higher frequencies.

Besides evolved PNe, the SKA will allow us to detect more objects in the rapid transition from post-AGB stars to PNe, like CRL 618. This is a critical phase, when the development and expansion of the ionisation front radically changes the physical conditions in the circumstellar environment (Umama et al., 2004; Cerrigone et al., 2008, 2011). This transition lasts for a small fraction of the post-AGB time (which amounts to some 10^3 yr), which makes it challenging to detect stars going through it. Again, the deeper survey obtainable with the SKA will find new transition stars by sampling a larger volume of our Galaxy. In this context, it must be noted that transition objects are often optically thick below 3 GHz, therefore high-frequency receivers will be necessary to characterize the nebulae by observing their optically-thin emission. The flux may increase by 1% per year or more, a variation readily detectable if the survey is repeated over a few years.

Post-AGB stars such as CRL618 commonly show jet-like outflows. The origin and driving is not clear but magnetic-driven models have recently come in vogue (Huarte-Espinosa et al., 2012), strengthened by synchrotron emission from one such jet (Pérez-Sánchez et al., 2013). The SKA can detect synchrotron components to the radio emission through its sensitivity and wide frequency band: this will test the shaping mechanisms operating in PNe. This is best done at 1 GHz.

Finally, the SKA can also measure the mass of the stellar remnants inside the PN. This is done indirectly, through the evolution of the radio flux density. The rate of heating of the central star (temperature increase in K/yr) is a very strong function of the stellar mass. For stars which have not yet reached their maximum temperature, the radio flux is expected to decrease by 0.01-0.1% per year, due to the decrease in number of ionizing photons (hotter stars have fewer photons as each photon carries more energy). The rate of change of the optically thin radio flux yields the stellar mass, to an accuracy of better than 5%. This has so far only been done for NGC 7027 (Zijlstra et al., 2008). The changes during the earlier evolution are faster (Cerrigone et al., 2011) but less deterministic. The SKA survey can detect a 0.1% change for PNe as faint as 10mJy, which brings the Galactic Bulge population in range. A deeper, targeted survey could go further.

These measurements will best be carried out at 4–6 GHz (Zijlstra et al., 1989; Aaquist & Kwok, 1990). One way to achieve the temporal sensitivity is to repeat the Galactic plane area of the SKA survey 5–10 times, which would also improve sensitivity.

4. Stellar Radio emission

4.1 General

Stars emit, in the radio band, a negligible fraction of their total luminosity. In the case of the quiet Sun the ratio between its radio and its bolometric luminosity is less than 10^{-12} . Nevertheless,

in many cases, radio observations are the only way to reveal and study astrophysical phenomena that play a fundamental role in our understanding of stellar evolution. This is the case of stellar magnetic fields, whose topology can be directly mapped via VLBI observations (e.g. Trigilio et al., 1993; Peterson et al., 2010) and its influence on energy amplification and subsequent release in stellar coronae can be investigated via the correlation between radio and X-ray emission and the statistics of stellar flares (Benz & Guedel, 2010, and references therein); of stellar winds, where the detection of thermal radio emission is widely used to determine the mass-loss rate in hot stars (Wright & Barlow, 1975; Panagia & Felli, 1975; Scuderi et al., 1998; Blomme, 2011) and has revealed to be particularly powerful when other diagnostics cannot be used, as in the cases of dust enshrouded objects (Umama et al., 2005)

The improvement of the observational capabilities have lead to the discovery of radio emission in a wide variety of stellar objects from all stages of stellar evolution. Broadly speaking, the brightest stellar radio emission appears to be associated with enhanced stellar mass-loss (winds, nebulae) in the cases of thermal emission (large emitting surface) or to magnetically-induced phenomena, such as stellar flares, for non-thermal emission processes (high brightness temperature). In the following we briefly illustrate some representative examples for each type of stellar radio emitters.

4.1.1 Thermal emitters

Thermal emission (bremsstrahlung emission) is expected from winds associated with massive stars, shells surrounding Novae and jets from symbiotic systems (O'Brien et al. 2015), class 0 pre-main sequence (PMS) stars and classical TTauri (White, 2004).

Massive stars play a fundamental role in the evolution of galaxies. They are among major contributors to the interstellar UV radiation and, via their strong stellar winds, provide enrichment of processed material (gas and dust) and mechanical energy to the interstellar medium. Moreover, mass-loss from massive stars is very important for stellar evolution and understanding the different types of SN explosion.

Typical mass-loss rate for OB stars is of the order of $10^{-6}M_{\odot}/yr$, with wind speeds of $(1-3) \times 10^3 km/sec$. More evolved massive stars include the classes of Luminous Blue Variables (LBVs) and Wolf-Rayet (WR). Luminous Blue Variables are massive evolved stars in an highly unstable state. Photometric and spectral variabilities are as characteristic for that phase as is a highly enhanced mass loss (up to few $10^{-4}M_{\odot}/yr$) in various wind phases in which the wind velocities alternate between slow and fast. WR are further evolved, hotter and more stable massive stars with similar strong mass loss. The strong mass-loss of both object classes lead to extreme obscuration, in some cases, of the stellar surface. The mass-loss rate of massive star winds can be in principle derived from continuum radio observations, which trace the ionized gas through its optically thick free-free emission, providing the distance to the source and the velocity of the wind are known. A stellar wind has a typical spectral signature in the radio related to the radial density gradient of the wind (Panagia & Felli, 1975).

Radio observations have been proven to be more efficient than usual diagnostics for ionized gas, such as H_{α} , because they don't suffer from extinction and are indeed the only way to probe ionized gas in very reddened objects, embedded in dense, dusty circumstellar material. However, while mass-loss rates from radio continuum observations have been routinely obtained from a large

number of objects, quite recently it was realized that canonical mass-loss rates from massive stars need to be revised downwards, mostly because the assumed stellar-wind model does not include the effect of clumping or porosity (Blomme, 2011).

4.1.2 Non-thermal emitters

Much of our knowledge of non-thermal emission from radio stars comes from the study of active stars and binary systems as a large fraction of them have been found to be strong radio sources (Slee et al., 1987; Drake et al., 1989; Umana et al., 1991, 1993, 1998). Both classes of star are characterized by a magnetically heated outer atmosphere and display all the manifestations of solar activity (spots, chromospheric active regions, coronal X-ray emission, flares). In binary systems the observed phenomenology is more extreme than in the solar case because of the forced rotation induced by tidal forces that contributes to generate a more efficient dynamo action. The radio emission arises from the interaction between the stellar magnetic field with mildly relativistic particles (Dulk, 1985, i. e. gyrosynchrotron emission) and is highly variable. Two different regimes are usually observed: quiescent periods, during which a basal flux density of a few mJy is observed, and active periods, characterized by a continuous strong flaring which can last for several days (Umana et al., 1995).

Non-thermal radio emission is also observed in Ultracool dwarf (UCDs). The class of UCDs consists of stellar objects located on the boundary with sub-stellar bodies such as gas giant planets, including fully convective, very low mass M stars (later than M6) and Brown Dwarf (BDs).

The recent discovery of intense radio emission pulses lasting a few minutes from a number of UCDs has changed the conventional way to interpret their coronal emission physics; such objects exhibit very low chromospheric H-alpha and coronal X-ray activity and, consequently, were expected to be radio quiet (McLean et al., 2012, and references therein). This detection has immense implications for our understanding of both stellar magnetic activity and the dynamo mechanism generating magnetic fields in fully convective stars. This manifestation of magnetic activity is a significant departure from the incoherent gyrosynchrotron emission model generally applied to cool stars and bears more resemblance to planetary auroral activity than coronal stellar activity, indicating a possible transition in activity at the end of the main sequence. The radio pulses are thought to be due to highly beamed electron cyclotron maser emission and thus provide an accurate measurement of magnetic field strength at the location of the emission. This has been successfully used to provide the first measurements of magnetic field strengths for L and T dwarfs (Berger et al., 2009; Hallinan et al., 2007; Route & Wolszczan, 2012).

In several UCDs, such coherent emission is periodic, with a period consistent with their respective rotational periods (Berger et al., 2009; Hallinan et al., 2007). The long-term stability of the radio emission also indicates that the magnetic field (and hence the dynamo) is stable over a long timescale. How such fields are created and sustained remains a mystery.

Another example of non-thermal radio emitter is the class of Magnetic Chemically Peculiar stars (CPs). They are B-A main sequence stars characterized by strong dipolar magnetic fields with axis tilted with respect to the rotational one (oblique rotator). There are no convective motions in their stellar envelopes, and the magnetic field is thought to be fossil, remnant of the dynamo fields generated in the pre main-sequence phase.

CPs can show radio continuum emission, variable with the rotational period, but stable in time (Leone & Umama, 1993). The current model assumes that particles of the stellar wind are accelerated in the current sheets at Alfvén radius, and then propagate in a thin magnetospheric layer toward the star, emitting gyrosynchrotron radiation (Trigilio et al., 2004; Leto et al., 2006). Radio observations at 1.4-2 GHz of the CP star CU Vir have revealed the presence of a coherent, highly directive, 100% per cent polarized radio emission component (Trigilio et al., 2000), interpreted as cyclotron maser. In the framework of the radio emission from CP stars, maser amplification can occur in annular rings above the pole, generating auroral radio emission similar to what has been detected in the planets of the solar system, including the Earth (Trigilio et al., 2011). The coherent emission is stable on a time-scale of more than 10 years and has been used as a marker of the rotation of the star, revealing changes of the rotational period (Trigilio et al., 2008). The well known topology of CPs magnetic fields makes this type of object a perfect template for studies of stellar magnetosphere, magnetoactive plasma, particle acceleration, and stellar spin-down.

4.2 Radio stars detection forecast

In the last years, a few hundreds of radio stars have been detected (Guedel, 2002) but nearly all of the detections are the results of targeted observations directed at small samples of stars thought to be likely radio emitters. Therefore, all the detections suffer from a strong selection bias as the targeted observations were aimed at addressing specific problems related to some kind of peculiarities observed in other spectral regimes. This approach has been proven to be quite productive but it is biased against discovering unknown, unexpected, or intrinsically rare objects, preventing a good knowledge of radio stars at the sub-mJy level. In Fig. 3, schematic continuum radio spectra of several classes of radio emitting stars are drawn. Fluxes have been derived assuming a typical radio luminosity (Seaquist, 1993; Umama et al., 1993; Guedel, 2002; Berger et al., 2005; Trigilio et al., 2008), and a typical distance for each different types of radio stars: 10 pc for flare stars and late M-L, 100 pc for active binary systems, 1 kpc for supergiants, OB and WR, 500 pc for CP stars. The flux density of the quiet Sun has been derived from the solar quiescent radio luminosity assuming a distance of 10pc. The spectral and sensitive characteristics of SASS1 and SKA-MID, in both phases SKA1 and SKA, have been also drawn. The sensitivity for SKA1 and SKA is obtained assuming an integration time of 1 hour. For SKA1, we assume that band 2, band 4 and band 5 will be available, while for the full SKA we assume the deployment of all five frequency bands.

Stellar winds and non-thermal radio emission from many active binaries, flare stars and PMS stars will be easily detected, within the considered distances, with an rms sensitivity of $2 \mu\text{Jy beam}^{-1}$ (SASS1), even during its early phase of deployment. With SKA1 we will be able to detect a quiescent Sun, but only if band 4 or 5 is used.

Another way to see this is to estimate, starting from the typical radio luminosity and assuming a limiting sensitivity, at what distance is possible to detect a star belonging to a particular class of radio emitting object. With the limiting sensitivity detectable flux density of SKA1-MID, for 10 minutes of integration time, all the WR, OB and stars and Symbiotic systems of the Galaxy can be detected, while CP, PMS, RSCVn and Supergiants could be seen up to the distance of the Galactic Center (GC). With the same integration time, SKA-MID will be able to detect almost all the above classes in the Milky Way, and probably in the nearby galaxies, providing sufficient angular resolution ($\leq 0.02''$), M Giant photospheres to the distance of the GC, flare stars and UCDS

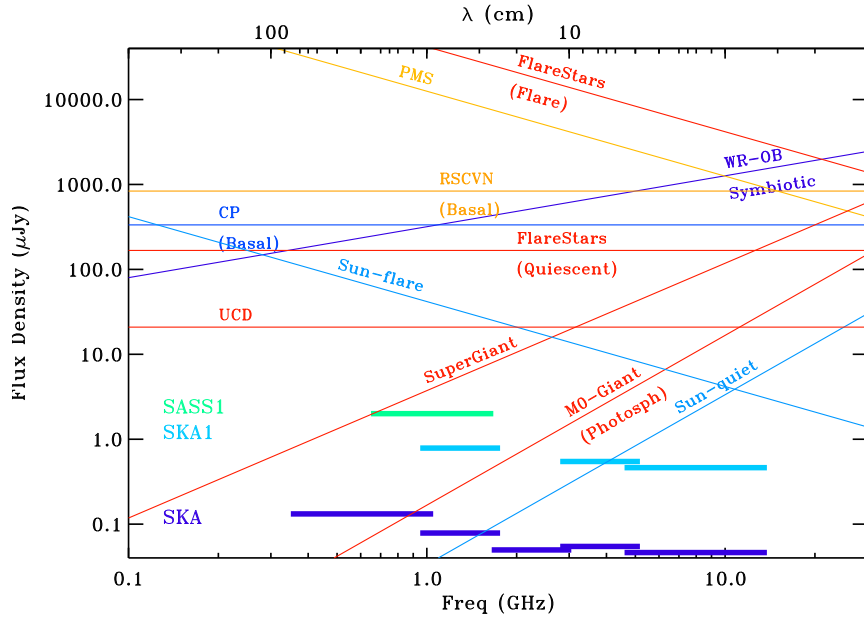


Figure 3: Typical radio spectrum of several classes of radio emitting stars. Fluxes have been derived from the radio luminosity assuming a distance as appropriate for each type of radio stars. Detection limits for SKA1 and SKA have been computed for one hour integration time. See text for explanation.

within several hundreds pc, and "a quiescent Sun analog" up to 50 pc (Fig. 4).

The unique capabilities of SKA will allow to detect many classes of stars over the entire Milky Way. This will produce a real revolution in stellar physics as the radio properties of different stellar populations will be defined, allowing timely comparisons with other stellar parameters, such as age, mass, magnetic fields, chemical composition, and evolutionary stages.

There are some particular areas of stellar radio emission that will particularly benefit from high sensitive and high angular resolution radio observations as those provided by the SKA. These are the study of non-thermal stellar flares in active stars and binary systems, the search for coherent events in different classes of stellar systems and the use of radio observations to derive mass-loss rate in massive stars.

It has not been established yet if the complete set of polarisation measurements (Stokes I, Q, U and V) will be available with both SKA1 and SKA foreseen observations. In particular circular polarisation information on a series of non-thermal radio emitting stars will complete our understanding of particular phenomena such as those related to coherent emission, allowing to immediately point-out coherent radio flares occurring in a particular target. However, most of the scientific goals, as reported in the following, could be reached even if only I, Q and U maps will be available.

4.2.1 Stellar Coronae: the solar-stellar connection:

In the Sun, during flares, beams of fast electrons travel down magnetic fields and release their energy in the chromosphere, where heated plasma expands into coronal magnetic flux tubes. This

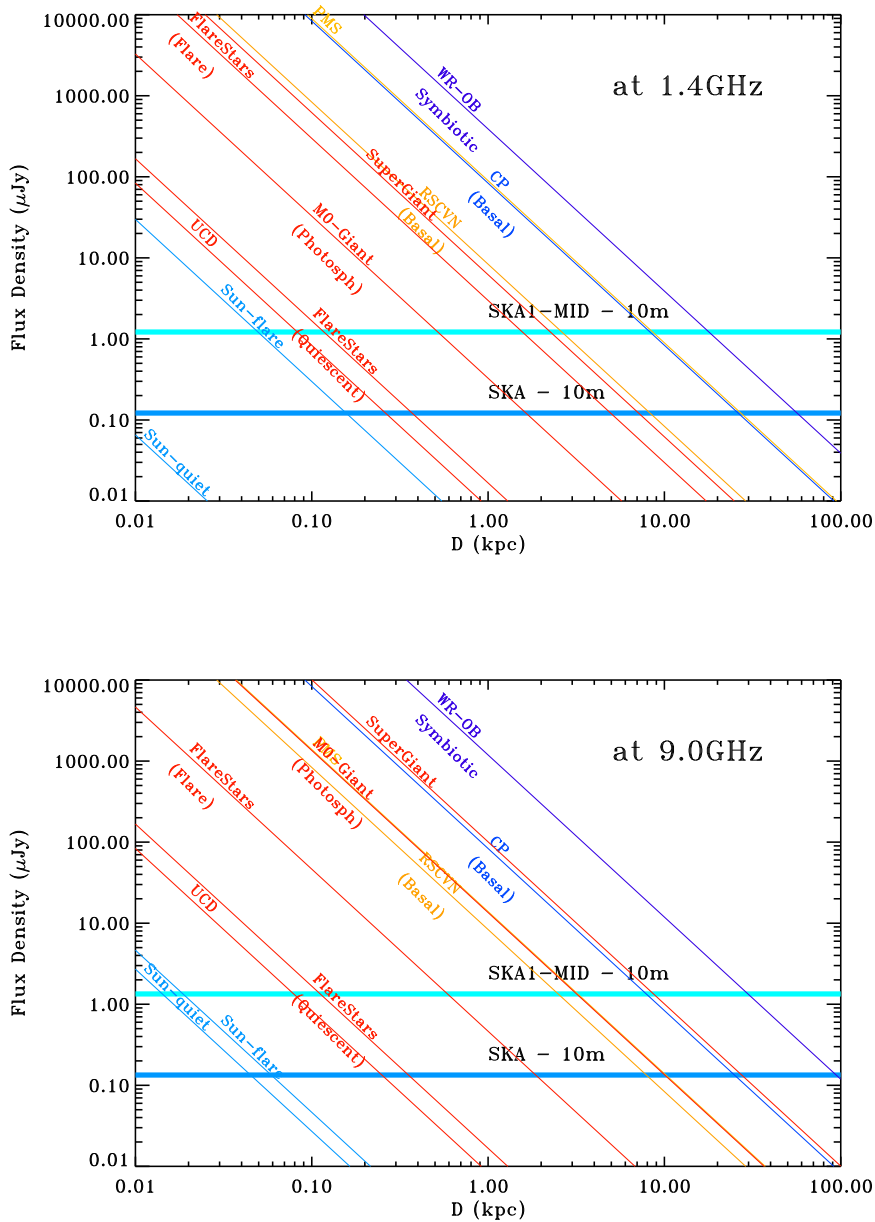


Figure 4: Top panel: Typical distances at which different classes of radio stars can be detected, assuming as limit flux the sensitivity that can be achieved with 10 minutes of integration band with SKA-MID in its band 2, in both SKA phase 1 and 2. **Bottom panel:** Same as top panel but for band 5.

hot plasma then cools radiatively and through conduction. Several attempts to use the solar model as a proxy to understand the energetics and location of flares in active stars have been carried out. Various theoretical mechanisms have been proposed, but more observations are clearly needed.

Until now, all the information on the radio emission from active stars and stellar systems originate from targeted observations of very few, bright, well known objects, usually selected on the basis of the strong magnetic activity displayed in other spectral regions.

Even if limited to a very small sample, we have now some knowledge of their radio emission characteristics (e.g. flare development, spectral and polarisation evolution, emission mechanism, etc). Deep radio measurements, as those that we can perform with SKA, would significantly enlarge the number of active stars and stellar systems, without bias effects, allowing new insights into the physics of objects showing magnetic activity. SKA1 would allow us to detect all the flares stars and active binary systems up to few kpc, while SKA will allow us to detect them over the whole Galaxy (Fig. 4) and thus to increase of two orders of magnitude the number of active stars that can be studied in the radio.

The study of large samples of active stars will provide us with important clues on stellar magnetism and dynamo processes as a function of internal structure of the stars and other physical parameters (mass, age, rotation...). Moreover, a clear understanding of the key parameters that control magnetic activity in different types of stars is very important since it affects habitability of possible orbiting planets.

It will be possible to identify radio coronae across a range of cool type stars. Detailed studies of a large number of stellar coronae will improve our knowledge of energy release in the upper atmospheres of stars of different mass and age. This will also permit to investigate the correlation between radio and X-ray emission and thus study the occurrence of the Neupert effect in stellar coronae (Guedel, 2009).

Systematic, multi-epoch deep surveys will enable the detection of serendipitous flaring activity and will hence permit to derive the typical behaviour (occurrence rate, evolution, etc.) from a statistical study of larger samples. Multi-wavelength type follow-up observing campaigns would allow to study magnetic activity manifestations at different layers of the stellar outer atmosphere and to explore the relationship of electron energization to the long-lived centers of surface activity (photospheric spots), pointing out the existence of possible magnetic cycles also in the radio.

Finally, the unique sensitivity of SKA will allow to follow the development of flares with unprecedented details and time-resolution. A typical, solar-type weak flare (0.1 mJy at 1.3 pc) can be detected in 5 sec with SKA1 (5σ). Such kind of observation will provide new insights in the open question of coronal heating and, in particular, a piece of evidence that the radio quiescent corona is maintained by a series of micro-flares.

4.2.2 Coherent events

There is a growing evidence that stellar radio flares can occur also as narrow band, rapid, intense and highly polarized (up to 100%) radio bursts, that are observed especially at low frequencies (<1.5 GHz). For their extreme characteristics, they have been generally interpreted as result of coherent emission mechanisms. such as the Electron Cyclotron Maser Emission (ECME). Coherent burst emission has been observed in different classes of stellar objects: RS CVns and

Flare stars (Osten & Bastian, 2008; Slee et al., 2008), Ultra Cool dwarfs (Hallinan et al., 2008; Route & Wolszczan, 2012) Chemically Peculiar stars (Trigilio et al., 2008, 2011), all having, as common ingredient, a strong and also, but not necessarily, variable magnetic field and a source of energetic particles. The number of stars where coherent emission has been detected is still limited to few tens, because of the limited sensitivity of the available instruments and the stochastic nature of the events.

Deep radio observations, such those that SKA will provide the best opportunity to determine how common coherent radio emission is from stars, stellar and sub-stellar systems. The detection of coherent emission in a large sample of different types of stars will have immense implications for our understanding of both stellar magnetic activity and the dynamo mechanism generating magnetic fields in fully convective stars and brown dwarfs (Hallinan et al., 2008; Ravi et al., 2011).

Coherent emission observed in binary systems and active stars and in UCD stars shares several characteristics with that observed in CP stars (Trigilio et al., 2000), since both require a large scale magnetosphere, and are similar to the low frequency coherent radio emission observed in the planets with magnetic field of the solar system (Trigilio et al., 2011). To better understand the ECM in the wider context of plasma processes it is necessary to extend radio observations to a larger sample of CP stars. We want to stress here that CP stars provide us with the unique possibility to study plasma processes in stable magnetic structures, whose topologies are quite often well determined by several independent diagnostics (Bychkov et al., 2005), thus overcoming the problem of variability of the magnetic field observed in very active stars such dMe or close binary systems.

The foreseen sensitivity of SKA, just in its first phase, will allow to detect CP stars up to 10 kpc in 10 minute integration time (Fig. 4). Following Renson & Manfroid (2009), we can assume the CP stars are uniformly distributed in space. This would imply that the number of radio detections will increase by about an order of magnitude, giving the opportunity to get a larger statistics of the physical conditions of the magnetospheres to be correlated to the ECM.

If coherent emission is present in many radio active stars, with the same characteristics, it will constitute an excellent diagnostic for star magnetospheres, and a powerful probe of magnetic field topology. In the case of UCDs the study of ECM instability provides the only potential probe into magnetic field strengths for late-M, L and T dwarfs.

More observations of wider samples of active stars are also necessary to establish the percentage of active stars and binary systems that show coherent emission, exploring time-scales of its variability and how this is related to the basic physical parameters of the stars. Follow-ups of the detected sample would allow to point-out any similarities between ECME from single stars and binary systems and thus discriminate between different causes for the population inversion that drives the ECME events (Slee et al., 2008).

The discovery of other radio lighthouses similar to those observed in CU Vir (Trigilio et al., 2008; Ravi et al., 2011) will enable high precision studies of the rotation period, and thus angular momentum evolution, in different classes of stars.

4.2.3 Mass-loss from Massive stars

The recent discovery that the mass-loss rates derived for hot main sequence massive stars need to be revised downwards (Blomme 2011), poses serious questions on the evolution of massive stars.

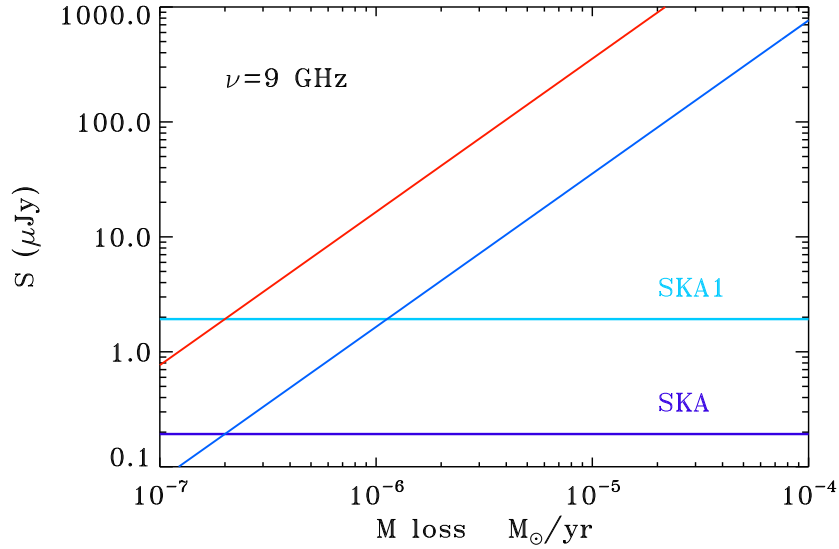


Figure 5: Mass-loss rates detectable at the distance of the Galactic Center (8 kpc) for two values of wind velocities. Sensitivity (rms), for 10 minute integration time for both SKA1 and SKA band 5, has been assumed.

An O-type star on the Main Sequence (MS), whose mass may be as large as $150 M_{\odot}$, will evolve into a Wolf-Rayet star, with a typical mass not in excess of $30 M_{\odot}$, but MS mass-loss rates are insufficient to account for such a huge mass-loss. Severe mass-loss probably occurs through strong stellar winds and/or eruptions during the post-MS evolution. Many luminous classes of stars belong to this phase, hot supergiants (BSGs, B[e]s and LBVs), cool Yellow Hypergiants (YHGs) and red Supergiants (RSGs) stars. The exact evolutionary path leading to a W-R, as a function of the mass and rotation, is however not well constrained, mostly because a crucial piece of information, i.e. mass-loss rates and lifetime and thus the total amount of mass lost during the post-MS is currently incomplete.

LBVs may play a key role in this scenario; as well as being characterized by a strong mass-loss, they can also undergo giant eruptions, in which larger amounts of mass are being ejected. As a consequence of the strong stellar wind and/or the giant eruption, circumstellar nebulae (LBVN) are formed (few M_{\odot} for the wind scenario, several M_{\odot} by ejection), which are a few parsec in size and have expansion velocities between 10-200 km/s, in extreme cases several 1000 km/s are detected (Weis, 2011). The nebulae are seen in optical and IR emission lines, radio continuum emission and IR excess emission. The possibility that such spectacular mass-loss events may be metallicity-independent has greatly increased the interest in LBVs, as this can have important implications for the mass-loss and therefore the evolution of Population III stars. Observations of LBV eruption and other variabilities of massive stars in local very low metallicity galaxies already hint at additional physics, which will improve the link from local massive stars to stars at the time of reionization (Bomans & Weis, 2011).

Mass-loss rates from a number of LBVs and LBVs candidates have been recently derived by

radio observation in our own Galaxy (Umana et al., 2005, 2010, 2012) and in the LMC (Agliozzo et al., 2012). Radio observations have also allow to determine the morphology of the ionized fraction of some LBVNs and to quantify the mass of ionized material (Buemi et al., 2010; Umana et al., 2011). When radio maps are combined with detailed mid-IR maps, tracing the dusty component, the presence of multi-epoch mass-loss events have been pointed out and estimates of the total content in mass of LBVNs have been derived (Umana et al., 2012; Agliozzo et al., 2014). Of further interest will be a comparison of the radio data with optical/NIR images of several LBVN. Weis (2011) showed that the morphology of LBVN as deduced from [NII] or H_{α} images and a kinematic analysis (Weis, 2003, i.e.) is bipolar in about 50% of all nebulae; for galactic LBVNs this rises to 75%. MIR dust nebulae appear to give different results, but are due to another driving mechanism, therefore radio observations are crucial for the understanding of formation and evolution of nebulae, e.g. determining the influence of wind-wind interactions and stellar rotation.

In Fig 5, the mass-loss rates detectable at the distance of the Galactic Center (8 kpc), assuming the SKA1 and SKA sensitivity with a 10 minute integration time, are shown. The red line refers to a wind velocity of 100km/sec , while the blue line to 1000km/sec . The minimum detectable flux has been calculated for SKA-MID band 5, as it is at higher frequency that we have the highest contribution from the optically thick, thermal stellar wind. Fig. 5 indicates that with the SKA, in both phases, we will reach, in 10 minute integration time, a detection limit sufficient to measure also very small mass-loss rates ($\sim 10^{-7} M_{\odot}\text{yr}^{-1}$) at the distance of the Galactic Center. This would allow studies, similar to those currently conducted on LBVs, to be carried out inside the three massive stellar clusters, located near the Galactic Center (Arches, Quintuplet and the Central Cluster). These young stellar clusters are more massive than any other cluster in the Milky Way and are likely to contain massive stars at all stage of evolution, including pre-main sequence, LBV and W-R, allowing to explore a plethora of stellar winds and associated Nebulae from a stellar population at the same age and, given the unique location, to study as these can be affected by environmental parameters.

References

- Aaquist, O. B., & Kwok, S. 1990, A&AS, 84, 229
Agliozzo, C., Umana, G., Trigilio, C., et al. 2012, MNRAS, 426, 181
Agliozzo, C., Noriega-Crespo, A., Umana, G., et al. 2014, MNRAS, 440, 1391
Anglada, G., Rodríguez, L.F., Carrasco-González, C., 2015, "Radio Jets in Young Stellar Objects with the SKA", in proceedings of "Advancing Astrophysics with the Square Kilometre Array", PoS(AASKA14)121
Arthur, S. J., & Hoare, M. G. 2006, ApJS, 165, 283
Benz A.O., Güdel, M., 2010, ARA&A, 48, 241
Berger E., Rutledge R.E., Reid I.N. et al., 2005, ApJ, 627,960
Berger E., Rutledge R.E., Phan-Bao N., et al., 2009, ApJ, 695, 310
Blomme, R. 2011, Bulletin de la Societe Royale des Sciences de Liege, 80, 67
Bychkov, V. D., Bychkova, L. V., & Madej, J. 2005, A&A, 430, 1143
Bomans, D. J., & Weis, K. 2011, IAU Symposium, 272, 265

- Braun, R., 2014, "SKA1 Imaging Science Performance", Document number SKA-TEL-SKO-DD-XXX Revision A Draft 2
- Buemi, C. S., Umama, G., Trigilio, et al. 2010, *ApJ*, 721, 1404
- Cerrigone, L., Umama, G., Trigilio, C., et al. 2008, *MNRAS*, 390, 363
- Cerrigone, L., Trigilio, C., Umama, G., et al. 2011, *MNRAS*, 412, 1137
- Ciardullo, R. 2010, *PASA*, 27, 149
- De Pree, C. G., Peters, T., Mac Low, M.-M., et al. 2014, *ApJ*, 781, L36
- Dewdney, P., Turner, W., Millenaar, R., McCool, R., Lazio, J., Cornwell, T., 2013, "SKA1 System Baseline Design", Document number SKA-TEL-SKO-DD-001 Revision 1
- Drake S.A., Simon T., Linsky J.L., 1989, *ApJS*, 71, 905
- Dulk, G. A. 1985, *ARA&A*, 23, 169
- Güdel, M., 2002, *ARA&A*, 40, 2017
- Güdel, M., 2009, *LNP*, 778, 269
- Hallinan G., Bourke S., Lane C., 2007, *ApJ*, 663, 25
- Hallinan G., Antonova A., Doyle J.G. et al., 2008, *ApJ*, 684, 644
- Helfand, D. J., Becker, R. H., White, R. L. et al., 2006, *AJ*, 131, 2525
- Hoare, M. G., Purcell, C. R., Churchwell, E. B., et al. 2012, *PASP*, 124, 939
- Hosokawa, T., Yorke, H. W., & Omukai, K. 2010, *ApJ*, 721, 478
- Huarte-Espinosa, M., Frank, A., Blackman, E. G., et al. 2012, *ApJ*, 757, 66
- Jacoby, G. H., Kronberger, M., Patchick, D., et al. 2010, *PASA*, 27, 156
- Keto, E. 2002, *ApJ*, 580, 980
- Keto, E. 2003, *ApJ*, 599, 1196
- Kurtz, S. 2005, *Astrochemistry: Recent Successes and Current Challenges*, 231, 47
- Leone F., Umama G., 1993, *A&A*, 268, 667
- Leto P., Trigilio C., Buemi C.S. et al., 2006, *A&A*, 458, 831
- McClure-Griffiths, N. M., Dickey, J. M., Gaensler, B. M., et al. 2005, *ApJS*, 158, 178
- McLean M., Berger E., & Reiners A., 2012, *ApJ*, 746, 23
- Mottram, J. C., Hoare, M. G., Davies, B., et al. 2011, *ApJ*, 730, L33
- Murphy, T., Mauch, T., Green, A., et al. 2007, *MNRAS*, 382, 382
- Norris, R. P., Hopkins, A. M., Afonso, J., et al., 2011, *PASA*, 28, 215
- Norris, R. P., Basu, K., Brown, M., et al., 2015, "The SKA Mid-frequency All-sky Continuum Survey: Discovering the unexpected and transforming radio-astronomy" in proceedings of "Advancing Astrophysics with the Square Kilometre Array", *PoS(AASKA14)086*
- O'Brien, T., Rupen, M., Chomiuk, L., et al., 2015, "Thermal radio emission from novae & symbiotics with the Square Kilometre Array" in proceedings of "Advancing Astrophysics with the Square Kilometre Array", *PoS(AASKA14)062*
- Osten R.A., Bastian T.S., 2008, *ApJ*, 674, 1078
- Panagia, N., & Felli, M. 1975, *A&A*, 39, 1
- Parker, Q. A., Acker, A., Frew, D. J., et al. 2006, *MNRAS*, 373, 79
- Pérez-Sánchez, A. F., Vlemmings, W. H. T., Tafoya, D. et al., 2013, *MNRAS*, 436, L79
- Peterson, W. M., Mutel, R. L., Güdel, M. et al., 2010, *Nature*, 463, 207
- Ravi V., Hobbs G., Wickramasinghe D. et al., 2010, *MNRAS*, 408, 99
- Ravi V., Hallinan G., Hobbs G. et al., 2011, *ApJ*, 735, L2

- Renson, P., & Manfroid, J. 2009, *A&A*, 498, 961
- Route, M., & Wolszczan, A. 2012, *ApJ*, 747, L22
- Scuderi, S., Panagia, N., Stanghellini, C. et al., 1998, *A&A*, 332, 251
- Seaquist E.R., 1993, *RPPh*, 56, 1145
- Slee O.B., Nelson G.J., Stewart R.T. et al., 1987, *MNRAS*, 229, 659
- Slee O.B., Willes A.J., Robinson R.D., 2003, *PASA*, 20, 257
- Slee O.B., Wilson W., Ramsay G., 2008, *PASA*, 25, 94
- Taylor, A. R., Gibson, S. J., Peracaula, M., et al. 2003, *AJ*, 125, 3145
- Trigilio, C., Umána, G., & Migenes, V. 1993, *MNRAS*, 260, 903
- Trigilio C., Leto P., Leone F., Umána G. et al., 2000, *A&A*, 362, 281
- Trigilio C., Leto P., Umána G., Leone F., Buemi C.S., *A&A*, 2004, 418, 593
- Trigilio C., Leto P., Umána G. et al., 2008, *MNRAS*, 384, 1437
- Trigilio C., Leto P., Umána G. et al., 2011, *MNRAS*, 739, L10
- Umána G., Catalano S., Rodonó M., 1991, *A&A*, 249,217
- Umána G., Trigilio C., Tumino M. et al., 1993, *A&A*, 267, 126
- Umána G., Trigilio C., Hjellming R.M. et al., 1995, *A&A*, 298, 143
- Umána G., Trigilio C., Catalano S., 1998, *A&A*, 329, 1010
- Umána, G., Cerrigone, L., Trigilio, C., & Zappalà, R. A. 2004, *A&A*, 428, 121
- Umána, G., Buemi, C. S., Trigilio, C. et al., 2005, *A&A*, 437, L1
- Umána, G., Buemi, C. S., Trigilio et al., 2010, *ApJ*, 718, 1036
- Umána, G., Buemi, C. S., Trigilio, C., et al. 2011, *ApJ*, 739, L11
- Umána, G., Ingallinera, A., Trigilio, C., et al. 2012, *MNRAS*, 427, 2975
- Wang, L., Cui, X., Zhu, H., Tian, W., 2015, "Investigations of supernovae and supernova remnants in the era of SKA", in proceedings of "Advancing Astrophysics with the Square Kilometre Array", PoS(AASKA14)064
- Weis, K. 2003, *A&A*, 408, 205
- Weis, K. 2011, *IAU Symposium*, 272, 372
- White, S. M. 2004, *New Astronomy Reviews*, 48, 1319
- Wood, D. O. S., & Churchwell, E. 1989, *ApJ*, 340, 265
- Wright, A. E., & Barlow, M. J. 1975, *MNRAS*, 170, 41
- Zijlstra, A. A., Pottasch, S. R., & Bignell, C. 1989, *A&AS*, 79, 329
- Zijlstra, A. A., van Hoof, P. A. M., & Perley, R. A. 2008, *ApJ*, 681, 1296